

LOW-MASS STAR FORMATION: INITIAL CONDITIONS, DISK INSTABILITIES, AND THE BROWN DWARF DESERT

CHRISTOPHER D. MATZNER^a AND YURI LEVIN^b

^aDepartment of Astronomy & Astrophysics

^bCanadian Institute for Theoretical Astrophysics

University of Toronto, 60 St. George Street, Toronto, ON M5S 3H8, Canada

Draft version February 7, 2020

ABSTRACT

We develop a simple theory to predict the initial conditions for low-mass star formation and relate these to instabilities of protostellar accretion disks that may produce stellar or substellar companions.

We first account for the effects of a turbulent velocity field on the cores that form stars. Revised scales for mass, radius, turbulent velocity, and angular momentum are derived from the gas temperature of the prestellar core and the column density of the parent cloud. The full distribution angular momentum around its characteristic scale is derived from an idealized but reasonable set of assumptions.

Second, we examine the criterion for fragmentation to occur during star formation, concentrating on the self-gravitational instabilities of protostellar accretion disks in their main accretion phase. Disk instability can develop from rotating initial conditions even if they are axisymmetric; therefore it provides a conservative bound for the criterion of fragmentation. Self-gravitational instabilities are strongly dependent on the thermal state of the disk, and we find that stellar irradiation quenches fragmentation due to Toomre's local instability. An early phase of fragmentation is nevertheless likely, but fragments born in this phase are in close proximity and are likely to merge later due to disk accretion. Global instability of the disk may be required to process mass supply, but this is unlikely to produce fragments. These conclusions help to explain the dearth of substellar companions to stellar type stars – the brown dwarf desert.

1. INTRODUCTION

At birth, stars accumulate their material through disks that are well known to be dense and massive. Both of these properties make protostellar accretion disks susceptible to self-gravitational instability (e.g., Toomre 1964). Indeed, simulations of protostellar disk accretion and evolution like those of Lin & Pringle (1990) typically find that they approach or cross the threshold for instability, either because of a high disk density or because of a finite disk mass. When this occurs, disk motions caused by self-gravity become important and perhaps dominant sources of angular momentum transport (Paczynski 1978; Lin & Pringle 1987; Papaloizou & Savonije 1991; Adams et al. 1989; Tohline 1994; Laughlin & Bodenheimer 1994; Gammie 2001). Indeed, they may be required for disks to process mass accretion.

Disk self-gravity is of interest not only as a transport mechanism, but also because it may cause the disk to fragment into self-gravitating bodies that can become stellar, substellar, or possibly planetary com-

panions to the star being formed.

If fragments form sufficiently early and survive as most of the stellar mass is accumulated, they stand a chance of acquiring mass comparable to that of the primary object (Bonnell 1994; Matsumoto & Hanawa 2003). Alternatively, fragments that survive but fail to accumulate material may wind up with brown dwarf or planetary masses at the end of accretion, depending partly on where in the disk they form. The possibility that gas giant planets form from fragmentation of a gaseous disk was suggested by Cameron (1978) and advocated by Boss (e.g., Boss 1997). It has been investigated numerically by Mayer et al. (2002), for example. Numerical investigations are difficult, both because of the high resolution required to attain convergence in self-gravitating simulations of cooling gas (Truelove et al. 1997), and because of the importance of thermal evolution to disk fragmentation (Nelson et al. 2000; Gammie 2001; Pickett et al. 2003; Rafikov 2004). We return to disks' thermal evolution below.

The possibility that disk instability can produce stellar or substellar companions makes it relevant to

the problem of binary and multiple star formation, and to the origin of the stellar initial mass function. The binary problem is reasonably well-posed, since the prestellar cores have been mapped (e.g., Benson & Myers 1989) and binary stars are also well studied. Indeed, binaries' angular momenta are similar to cores' (Duquennoy & Mayor 1991; Boss et al. 2000), a fact that explains some trends in binary properties Fisher (2004). However the mechanism by which a core fragments is currently unclear. It is not understood, for instance, why some stars – albeit less than half – form on their own.

Tohline (2002) has reviewed theories for the origin of binary stars, and identified three leading mechanisms: “prompt” fragmentation in a sheet formed from the quasi-homologous collapse of a cold, rotating cloud; fission of a rapidly rotating and contracting protostar, and self-gravitational instabilities of accretion disks. (Hoyle's 1953 proposal of opacity limited fragmentation during collapse appears unlikely, due to pressure gradients caused by central concentration of the initial state.) One should add to Tohline's list *turbulent* fragmentation, in which nonlinear perturbations in the initial state engender fragments directly; see Padoan & Nordlund (2002) and Klein et al. (2003).

Given the turbulence that characterizes the molecular clouds from which stars form, one might wonder how relevant axisymmetric instabilities can possibly be to stellar fragmentation. However, note the energy in this turbulence is concentrated in its longest wavelengths (Larson 1981). The direct progenitors of single and binary stars are the dense molecular cores which are supported significantly by thermal pressure, unlike the larger structures that contain them – their parent cloud or the cloud substructures known as clumps – which are supported entirely by turbulence and magnetic fields (McKee et al. 1993). On the scale of an individual prestellar core, perturbations with longer wavelength appear as translational motion, shear, and overall compression. All of these can be treated with an axisymmetric model in the center of mass frame. Motions with smaller wavelengths constitute turbulence within the core and contribute to turbulent fragmentation but are weaker in general and are suppressed by ion-neutral friction (Zweibel & Josafatsson 1983). For these reasons, and for analytical convenience, we will concentrate on axisymmetric initial conditions.

In this paper we develop a simple axisymmetric description of the initial conditions of star formation and examine the susceptibility of the predicted protostellar accretion disks to several modes of gravitational fragmentation. We begin by modeling the effect of molecular cloud turbulence on the masses,

radii, and rotation rates of the prestellar molecular cores (§ 2). We then address the “prompt” instability that occurs early in the collapse (§ 3), using criteria developed by the numerical survey of Matsumoto & Hanawa (2003). This analysis suggests that fragmentation occurs quite frequently in the early collapse, but we argue that the fragments so formed may merge during subsequent accretion.

We then turn (§ 4) to fragmentation due to Toomre (1964)'s instability. Since this is governed by the local density, we will call it “local fragmentation”. Here we must discriminate between conditions in which Toomre's instability saturates, inducing angular momentum transport (Paczynski 1978; Lin & Pringle 1987; Papaloizou & Savonije 1991; Laughlin & Bodenheimer 1994; Laughlin & Rozyczka 1996), and conditions that lead to local fragmentation. For this we rely on Gammie (2001), who identified the boundary between saturated “gravitoturbulence” and fragmentation in his simulations of razor-thin accretion disks. Although protostellar disks are hardly razor-thin, Gammie's criterion is a useful litmus test for fragmentation. It demonstrates that the outcome of gravitational instability is sensitive to the thermal evolution of the disk midplane, which we model first by treating only viscous heating alone in §4.1.1. This analysis indicates the possibility of fragments forming with periods greater than about 350 years. However, when we account for irradiation from the central star in §4.2, we will demonstrate that this quenches local fragmentation in the main accretion phase.

Next we treat instability that arises from the finite disk mass (Adams et al. 1989; Tohline 1994). This sets in if other transport mechanisms fail to flush the disk. However it is not yet clear whether such global instability can cause fragmentation (e.g., Bonnell 1994), or will always redistribute disk material sufficiently to quench itself (Laughlin et al. 1998; Laughlin & Rozyczka 1996).

We draw conclusions in §6.2 about the implications of this work for understanding the brown dwarf desert, i.e., the observed underrepresentation of sub-solar companions to solar type stars.

2. STAR FORMATION: INITIAL CONDITIONS

Prior to their collapse, molecular cores are partially supported by thermal pressure and are confined by the hydrostatic pressure of their parent cloud and permeated by its turbulent motions. Combined with the scalings known to apply to molecular cloud turbulence, these statements suffice to predict, if only crudely, the initial conditions for star formation. See also McKee (1999) and McKee & Tan (2003).

First, consider the structure of cores prior to their

collapse. In the absence of non-thermal pressure from magnetic fields, turbulence, or rotation, these are Bonnor-Ebert (BE; Bonnor 1956) spheres, confined by some external pressure P . They exhibit a sequence of increasing self-gravity and central concentration, leading up to a critical state whose mass and radius satisfy

$$M_{\text{BE}} = 1.18 \frac{\sigma_{\text{th}}^4}{G^{3/2} P^{1/2}} \quad \text{and} \quad \frac{M_{\text{BE}}}{R_{\text{BE}}} = 2.43 \frac{\sigma_{\text{th}}^2}{G}, \quad (1)$$

where σ_{th} isothermal sound speed. Molecular line cooling and dust radiation typically conspire to maintain $\sigma_{\text{th}} \simeq 0.2 \text{ km/s}$, corresponding to temperatures $T \simeq 10 \text{ K}$ for molecular gas (Fuller & Myers 1993); however one can imagine other possibilities, such as star formation in strongly heated or metal-free gas, in which T could be significantly higher.

Because non-thermal forms of pressure also contribute, it is reasonable to replace σ_{th} with an effective sound speed c_{eff} derived below. The Bonnor-Ebert parameters M_{BE} and R_{BE} provide fiducial values for the core mass and radius, although the actual values (M_c and R_c , say) differ because $c_{\text{eff}} > \sigma_{\text{th}}$. We show below that thermal and nonthermal contributions are comparable in these objects.

Goodman et al. (1993) and Burkert & Bodenheimer (2000) have shown that the observed rotation rates of molecular cores are consistent with the turbulent velocity fields of their parent clouds, if extrapolated to the sizes of individual cores. It follows that σ_{NT} for an individual core can be predicted the same way.

Unlike cores, molecular clouds are supported by a triumvirate of turbulent velocity, turbulent magnetic fields (which together compose σ_{NT}) and magnetic field pressure, with σ_{th} being entirely negligible on scales above R_c . Clouds are famously reported to obey a line width-size relation, noted first by Larson (1981) and refined by Solomon et al. (1987), in which

$$\sigma_{\text{NT}}(R)^2 \simeq 0.70 G \Sigma_{\text{cl}} R, \quad (2)$$

corresponding to a state of strong self-gravity (McKee 1999). In (2), R refers to the scale on which σ_{NT} is measured – on the core scale, σ_{NT} would be $\sigma_{\text{NT}}(R_c)$.

The column density of the parent cloud or molecular clump is Σ_{cl} ; Solomon et al. (1987) find, using a virial analysis, that for giant molecular clouds Σ_{cl} is remarkably constant around the value $165 M_{\odot}/\text{pc}^2$. However, Σ_{cl} does depend on context: in M33, for example, Rosolowsky et al. (2003) derive $\Sigma_{\text{cl}} \simeq 120 M_{\odot}/\text{pc}^2$; in the LMC, P et al. (1998) derive $\Sigma_{\text{cl}} \sim 700 M_{\odot}/\text{pc}^2$ ($\pm 0.3 \text{dex}$); and in Galactic clumps forming massive stars (Plume et al. 1997; McKee & Tan 2003) or in extragalactic starburst regions (e.g., Sargent & Scoville 1991; Scoville et al. 1991), $\Sigma_{\text{cl}} \sim 3000 - 5000 M_{\odot}/\text{pc}^2$.

The confining pressure for a core must derive from the mean hydrostatic pressure of the parent clump or cloud; this is (McKee 1999)

$$P = 0.51 f_p G \Sigma_{\text{cl}}^2. \quad (3)$$

where we have included f_p to account for variations in clump or cloud structure (0.51 refers to a spherical cloud with $\rho \propto 1/r$ and no embedded stars) and for fluctuations around the mean value due to turbulence or location within the cloud. With equations (1), this implies

$$\begin{aligned} M_{\text{BE}} &= 2.36 \frac{\sigma_{\text{th}}^4}{G^2 \Sigma_{\text{cl}}} = \frac{0.70}{f_p^{1/2}} \frac{165 M_{\odot} \text{pc}^{-2}}{\Sigma_{\text{cl}}} T_{\text{eff},10}^2 M_{\odot}, \\ R_{\text{BE}} &= 0.97 \frac{\sigma_{\text{th}}^2}{f_p^{1/2} G \Sigma_{\text{cl}}} = \frac{0.034}{f_p^{1/2}} \frac{165 M_{\odot} \text{pc}^{-2}}{\Sigma_{\text{cl}}} T_{\text{eff},10 \text{pc}} \end{aligned} \quad (4)$$

where $T_{\text{eff},10}$ is the temperature for which $\sigma_{\text{th}} = c_{\text{eff}}$, measured in units of 10 K.

Now, let us compare $\sigma_{\text{NT}}(R_{\text{BE}})$ to σ_{th} . Combining equations (1), (2), and (3), one finds a turbulent contribution

$$\frac{\sigma_{\text{NT}}}{c_{\text{eff}}} = \frac{0.69}{f_p^{1/4}}, \quad (5)$$

independently of c_{eff} and Σ_{cl} .

The similarity between σ_{NT} and c_{eff} is not surprising: equations (2) and (3) describe cloud material as turbulence-supported and self-gravitating on all scales, whereas eq. (1) describes cores as supported by thermal motions. To be consistent, both thermal and nonthermal support must contribute about equally. The two rules must therefore agree on the characteristic column densities of cores; indeed, they give

$$\frac{M_{\text{BE}}}{\pi R_{\text{BE}}^2} = 1.1 f_p^{1/2} \Sigma_{\text{cl}}. \quad (6)$$

Equation (6) is not a surprise, since any self-gravitating object whose internal pressure is determined by the surface pressure must have a column density comparable to that of its parent self-gravitating clump or cloud; McKee & Tan (2003) find a relation quite similar to eq. (6) for turbulence-supported cores.

Likewise, the thermal and nonthermal predictions for the core's effective sound speed must be comparable. Although the numerical value 0.69 in eq. (5) depends on the details of the transition from thermal to turbulent support, equation (5) indicates that turbulence cannot be entirely negligible in pre-stellar cores. At the same time, it need not dominate their support.

To be specific, we adopt¹

$$c_{\text{eff}}^2 = \sigma_{\text{th}}^2 + 1.06\sigma_{\text{NT}}^2 \quad (7)$$

motivated by McKee & Holliman (1999)'s analysis of the mass of regions supported by Alfvén waves (treated in the WKB approximation: McKee & Zweibel 1995). With this, equation (5) is solved if

$$\sigma_{\text{NT}} \simeq \frac{0.98}{f_p^{1/2}} \sigma_{\text{th}}, \quad T_{\text{eff}} \simeq \frac{2.02}{f_p^{1/2}} T_c, \quad (\text{cores}) \quad (8)$$

which are power-law fits to the algebraic solution (good to 20% for $0.5 < f_p < 3$). Cores are therefore somewhat larger than objects lacking turbulent support:

$$\begin{aligned} M_c &\simeq \frac{4.1}{f_p} M_{\text{BE}} = \frac{2.8}{f_p^{3/2}} \frac{165 M_{\odot} \text{pc}^{-2}}{\Sigma_{\text{cl}}} T_{10}^2 M_{\odot}, \\ R_c &\simeq \frac{2.0}{f_p^{1/2}} R_{\text{BE}} = \frac{0.069}{f_p} \frac{165 M_{\odot} \text{pc}^{-2}}{\Sigma_{\text{cl}}} T_{10} \text{ pc} \end{aligned} \quad (9)$$

These values are more consistent with observations than R_{BE} and M_{BE} , which points to the presence of turbulent support. The fact that M_c exceeds the mean stellar mass is no concern: Matzner & McKee (2000) have shown that low-mass stars form at an efficiency $\varepsilon \simeq 25\% - 80\%$, due to the action of protostellar winds. Bear in mind, moreover, that there is a mass spectrum of cores going to larger and smaller masses, which generally resembles in its shape the stellar initial mass function (Motte et al. 1998).

It is also worth stressing that the objects we call "cores" are only the smallest and most thermally-supported self-gravitating regions identifiable within molecular clouds. The clumps that form clusters of stars, and clouds themselves, have $\sigma_{\text{NT}} \gg \sigma_{\text{th}}$ and masses much greater than M_c .

We have not yet specified the distribution of the variable f_p that determines cores' bounding pressures in comparison to the cloud or clump mean pressure. This is a product of several factors: the distribution of pressure within a cloud; the distribution of pressure with time due to turbulent fluctuations; and the likelihood of forming an unstable core, which presumably biases the distribution to higher pressures. On the other hand, the f_p distribution is strongly constrained if one posits that stars always form from marginally stable, thermally-supported cores whose masses are given by equation (9). In that case, the stellar initial mass function is a direct consequence

¹The coefficient of σ_{NT}^2 in eq. (7) depends on how c_{eff} is used. For Alfvén waves treated as a gas with adiabatic index 3/2 and polytropic index 1/2, this coefficient is 3/2 for $P = \rho c_{\text{eff}}^2$ (McKee & Zweibel 1995), 2/3 for $M_{\text{BE}} = 1.18 c_{\text{eff}}^3 / [G^{3/2} \rho(\text{edge})^{1/2}]$ (McKee & Holliman 1999), and 1.06 for $M_{\text{BE}} = 1.18 c_{\text{eff}}^4 / (G^{3/2} P^{1/2})$.

of the core mass distribution: $M_c \propto \varepsilon f_p^{-3/2}$. Conversely, the distribution of f_p is empirically determined, in such a theory, by the distribution of stellar (and binary) masses. For instance, Padoan et al. (1997) attribute the stellar initial mass function to the statistical distribution of pressure in simulations of supersonic, isothermal, unmagnetized turbulence. We will not adopt this strategy for the distribution of f_p , however, for two reasons. First, such a theory predicts that the most massive stars form in the lowest-density regions, which contradicts observations. Second, cores that create massive stars are significantly more massive than M_{BE} and therefore highly turbulent (e.g., McKee & Tan 2003). We reiterate that we consider only the typical, low-mass cores, for which thermal support is naturally significant.

We have not considered static magnetic fields in our treatment of cores; we comment on this in §2.4.

2.1. Core Rotational Properties

We follow Burkert & Bodenheimer (2000) and Fisher (2004) in assuming that the velocity field is homogeneous and Gaussian random with a spectrum consistent with equation (2). These authors also assume the components of \mathbf{v} to be uncorrelated, reducing the mean vorticity relative to an incompressible velocity field of the same σ . We shall first adopt the assumption of uncorrelated velocity components, then consider how the result should be modified to account for gas pressure.

Because both σ_{NT} and the specific angular momentum j derive from \mathbf{v} , one expects j to scale as $R_c \sigma_{\text{NT}}(R_c)$, and to show statistical fluctuations about this value. This expectation is borne out in the Appendix, where we compute the full distribution of j . Equations (A19) and (A20) imply, for a velocity field with uncorrelated components,

$$\begin{aligned} j &= 0.34 f_j R_c \sigma_{\text{NT}} \\ &= 2.3 \times 10^{21} f_j \left(\frac{\Sigma_{\text{cl}}}{165 M_{\odot} \text{pc}^{-2}} \right)^{1/2} \left(\frac{R_c}{0.1 \text{ pc}} \right)^{3/2} \frac{\text{cm}^2}{\text{s}} \\ &\simeq 1.3 \times 10^{21} \frac{f_j}{f_p^{3/2}} T_{10}^{3/2} \frac{165 M_{\odot} \text{pc}^{-2} \text{cm}^2}{\Sigma_{\text{cl}}} \frac{1}{\text{s}} \end{aligned} \quad (10)$$

where the last line uses R_c from equation (9).

Since we have assumed \mathbf{v} to be scale free, f_j is chosen from a distribution that depends only on the internal structure of the core, the turbulent spectral slope, and any correlations between components of \mathbf{v} . As explained in §A.2, j is distributed as a Maxwellian, or, crudely,

$$\log_{10} f_j = 0_{-0.49}^{+0.16}. \quad (11)$$

The above results pertain to velocity fields with strictly uncorrelated components, which is not entirely realistic. An uncorrelated flow can be decomposed into an irrotational, potential, compressive portion and a vortical, incompressive portion. In Fourier space, potential flows are aligned with the wavevector and vortical flows are perpendicular to it. Since there are twice as many degrees of freedom in the perpendicular direction, an uncorrelated flow contains two-thirds of its power in vortical motion and one-third in potential flow. Since core angular momentum derives entirely from the vortical part of the flow, it is $\sqrt{3/2}$ times higher in incompressible turbulence as compared to uncorrelated turbulence of the same σ . Equation (8) implies turbulent Mach numbers of about unity on the core scale, suggesting behavior intermediate between the incompressible and pressureless limits. It is reasonable, therefore, to multiply f_j by 1.11 (the harmonic mean of $\sqrt{3/2}$ and unity) to account for correlations introduced by pressure. This correction is however rather minor.

2.2. Collapse of Cores

Cores collapse with the accretion rate characteristic of any self-gravitating body, $\dot{M} = c_{\text{eff}}^3/G$ (Shu 1977). We assume only a fraction ε of the core successfully accretes, so the final stellar mass is $M = \varepsilon M_c$, and

$$\begin{aligned}\dot{M}_{\text{acc}} &\simeq \varepsilon \frac{c_{\text{eff}}^3}{G} \\ &= \frac{2.8 \times 10^{-6}}{f_p^{3/4}} \frac{\varepsilon}{60\%} T_{10}^{3/2} M_{\odot} \text{ yr}^{-1}\end{aligned}\quad (12)$$

There exists an initial phase of more rapid accretion during which the central region of the core collapses homologously; however, eq. (12) is valid for most of the mass.

The theory predicting $\varepsilon \sim 25\% - 80\%$ (Matzner & McKee 2000) invokes the removal of material from the rotational axis by protostellar jets; this somewhat increases the mean angular momentum of accreting material, but we make no correction for this effect.

The characteristic disk radius formed during infall is $j^2/(GM)$, or

$$R_d \simeq \frac{f_j^2}{45\varepsilon f_p^{1/2}} R_c = 230 T_{10} \frac{f_j^2}{f_p^{3/2}} \frac{60\%}{\varepsilon} \frac{165 M_{\odot} \text{ pc}^{-2}}{\Sigma_{\text{cl}}} \text{ AU.}\quad (13)$$

This is comparable to the critical radius beyond which the disk's self-gravity can cause local fragmentation, at least in principle; see equation (28) below. The maximum disk period is of order 9000 years, but is quite sensitive to the parameters f_j , ε , and f_p .

2.3. Comparison to Prior Models

We have not attempted to model the internal structures of cores under the influence of both thermal and nonthermal support, as previous authors have done (Myers & Fuller 1992; McKee & Holliman 1999; Curry & McKee 1999). Our emphasis has instead been on the overall mass, radius, and angular momentum scales of the smallest collapsible objects that can exist in a given turbulent environment. For this we rely on a Bonnor-Ebert model, rescaled to account for nonthermal support, and neglect the flattening of the density profile this nonthermal pressure should provide. Although far from perfect, this approximation is best for the most thermally-supported cores on which we concentrate.

In our study of core rotation we have followed Burkert & Bodenheimer (2000) in positing a homogeneous turbulent velocity field obeying the line width-size relation (2) that pervades cores and gives them rotation. Studies of core internal structure have often assumed instead that the nonthermal pressure is a function of the local density, e.g., in constructing multi-pressure polytrope (McKee & Holliman 1999) or nested polytrope (Curry & McKee 1999) core models, or that it is a function of the local core radius (Myers & Fuller 1992). Polytropic models are motivated, in part, by the polytropic behavior of Alfvén wave pressure in the WKB approximation (McKee & Zweibel 1995). This is an idealization because of the predominance of long-wavelength perturbations and because numerical simulations (e.g., Stone et al. 1998; Mac Low 1999) indicate that Alfvén waves damp rapidly in molecular cloud conditions. Our assumption of homogeneous turbulence is equally idealized: it does not explain the origin of the turbulent field, and it ignores the existence of a line width-density relation. We also have not accounted for the possibility of a break in the line width-size relation on scales between the core and its parent clump or cloud. Nevertheless, our results are in reasonable agreement with observations (§2.4).

Our model is similar in some ways to the TNT (thermal plus nonthermal) model introduced by Myers & Fuller (1992) and used recently by McKee & Tan (2003). However the TNT model posits a nonthermal line width that depends on the local radius from the core center: it is akin to the polytropic models in that it associates turbulence with the local conditions. The TNT model also idealizes core density structures as singular power laws, rather than accounting for the flat central region that exists prior to collapse: this is significant because it implies that thermal pressure will always dominate within some radius. In contrast, our models argue for comparable thermal and nonthermal contributions even in

maximally thermal cores.

Our predictions for the mass and radius of precollapse cores, equations (9), are similar to those of the smallest (thermal) cores in McKee & Tan (2003)'s theory. However these authors do not account for the possibility of a minimum level of turbulent support. As a result, their thermal cores are less massive and more slowly accreting than we would predict. Although Myers & Fuller and McKee & Tan do not address the core angular momentum distribution, their thermal cores would be significantly more quiescent and more slowly rotating than the cores modeled here. This difference is critical to questions of binary fragmentation.

2.4. Comparison to Observations

The mass and radius scales derived in §2 are consistent with the typical properties of prestellar cores observed in nearby star-forming regions, like Orion B (Johnstone et al. 2001). The core mass spectrum in such surveys typically shows a power law to masses above the minimum thermally-supported mass identified in this section. These authors identify an effective temperature using Bonnor-Ebert models which is typically 20-40 K, and note that some of these clumps have measured gas temperatures less than 20 K. A significant contribution of nonthermal pressure – as in our equation (8) – offers an explanation for this discrepancy.

Motoyama & Yoshida (2003) review a range of observational evidence that mass accretion can significantly exceed the characteristic value c_s^3/G in an early (class 0) accretion phase. They suggest the initial phase of homologous collapse, or collapse induced by an external impulse (see also Hennebelle et al. 2003), as possible explanations. These possibilities are both very reasonable, but note that we predict an accretion rate of roughly $2.6c_s^3/G$, on account of the nonthermal support (eq. [12]). Therefore, the need to invoke alternative explanations for the observed protostellar accretion rates is partially alleviated.

As for core rotation rates, equation (10) agrees with the value $j \sim 10^{21} \text{ cm}^2 \text{ s}^{-1}$ deduced by Goodman et al. (1993) for cores of similar mass. The second line differs from Burkert & Bodenheimer (2000)'s formula $j = 7 \times 10^{20} (R_c/0.1\text{pc})^{3/2} \text{ cm}^2 \text{ s}^{-1}$. However, Burkert & Bodenheimer 2000's results were numerical; our own unpublished numerical experiments, which were based on their method, have uncovered a bias to underestimate j by about the same factor.

Finally, we comment on the neglect of static magnetic fields in our calculations. Employing the Chandrasekhar-Fermi method, Crutcher et al. (2004) find that static magnetic fields in prestellar cores

could either be subdominant or comparable in magnitude with thermal pressure, depending on the application of a geometrical correction factor to their observations. Theoretically, one expects that ambipolar diffusion will sap the influence of magnetic fields prior to core collapse. In addition, observational inferences of short core lifetimes (Visser et al. 2002) are taken to indicate that static magnetic fields are not significant in core support. We conclude that our approximation of zero mean field is adequate given current uncertainties, while recognizing that this should be re-examined in future work.

3. PROMPT FRAGMENTATION

The first opportunity for fragmentation is in the initial phase of collapse, which follows from the homologous contraction of the core's central region. In this phase, the mass accretion rate can exceed equation (12). If the core's central region rotates sufficiently rapidly, it will form a disk that can fragment.

This phase of fragmentation has been studied in detail recently by Matsumoto & Hanawa (2003), who consider the initial collapse of slowly rotating Bonnor-Ebert spheres. Matsumoto & Hanawa find that fragmentation occurs by one mode or another so long as $\Omega_c t_{\text{ff,ctr}} \gtrsim 0.045$, where Ω_c is the rotation rate and $t_{\text{ff,ctr}}$ is the free-fall time evaluated at the middle of the initial state. Using equations (9), (10), and the moment of inertia $I_c = 0.2827 M_c R_c^2$, we find

$$\Omega_c t_{\text{ff,ctr}} \simeq 0.25 \frac{f_j}{f_p^{1/4}}. \quad (14)$$

By this criterion, then, all but the most slowly rotating cores ($f_j < 0.18 f_p^{1/4}$; about 3% of the population according to eq. [A20]) should undergo fragmentation in the initial collapse phase.

However, this conclusion is not robust. Note, first, that Matsumoto & Hanawa (2003) rely on the approximation of barotropic core collapse (isothermal, for $n_H < 10^{13} \text{ cm}^{-3}$) rather than a detailed thermodynamic calculation. Boss et al. (2000) caution that codes employing the Eddington approximation differ significantly from barotropic codes in their fragmentation patterns.

Second, Matsumoto & Hanawa's calculations stop after at most $0.07 M_\odot$ of several M_\odot have accreted into fragments. As they point out, the future evolution of these fragments is difficult to predict; in general, their orbits will tighten and potentially coalesce as they interact with material further out.

For both of these reasons we take equation (14) as only an indication that fragmentation may occur in the initial, impulsive collapse phase, and probe fragmentation in later stages of accretion in the upcoming sections. We consider disk thermodynamics in some

detail in §§4.1.1 and 4.2, where we calculate the instability of disks in the later phase of evolution during which equation (12) holds.

4. STEADY PROTOSTELLAR DISKS: LOCAL GRAVITATIONAL INSTABILITY AND LOCAL FRAGMENTATION

We now explore the stability of the steady protostellar accretion disks that form during the collapse of cores like those described in §2, during the phase of main accretion during which the accretion rate is given by (12). There are two modes by which self-gravitation can trigger disk fragmentation, one of which is subject to a local instability criterion (Toomre 1964) and the other a global one (Shu et al. 1990). We focus initially on the local instability and return to the global one in §5. The consequences of Toomre’s instability have been greatly elucidated by the numerical simulations of Gammie (2001), as described below.

Lin & Pringle (1990) have carried out an analysis of protostellar disk evolution, based on initial conditions qualitatively similar to those sketched in §2. They implemented a gravitational viscosity that rose as Toomre’s instability parameter,

$$Q \equiv \frac{c_s \Omega}{\pi G \Sigma}, \quad (15)$$

declined through its critical value of unity. (Here c_s , Ω , and Σ are the disk’s midplane isothermal sound speed, orbital frequency, and column density.) With this prescription for angular momentum transport, they found Q saturating typically in the range 0.2–0.5. This study lacked, however, two physical important physical effects: 1. the nonlocal nature of gravitational angular momentum transport when $Q > 1$; and 2. the dissolution into fragments of disks with $Q \lesssim 1$. Both shortcomings are addressed by the nonlinear simulations of Laughlin et al. (1998) and Gammie (2001):

1. When gravitational instability is weak and $Q > 1$, spiral modes saturate at low amplitudes via mode-mode coupling (Laughlin et al. 1998); in this state, redistribution of angular momentum is non-local and is described only approximately by a local prescription, i.e., by Shakura & Sunyaev’s α parameter (Laughlin et al. 1998). On the other hand, strongly unstable disks enter a state of “gravitoturbulence” (Gammie 2001) in which the coherence length is only a few effective scale heights

$$H \equiv \frac{c_s}{\Omega}.$$

In this state angular momentum transport is a local process (see also Lodato & Rice 2004). At the brink

of fragmentation, Shakura & Sunyaev’s viscosity parameter α takes its maximal value,

$$\alpha \simeq \frac{1}{3}. \quad (Q = 1) \quad (16)$$

We recall that α is related to the mass accretion rate through the disk:

$$\dot{M}_{\text{visc}} = \frac{3\pi\alpha\Sigma c_s^2}{\Omega}. \quad (17)$$

The subscript “visc” is added to distinguish the accretion rate due to local viscous transport from, for instance, the rate of mass supply (eq. [12]). Goodman (2003) points out that angular momentum loss in magnetized winds can lead mass to accrete more rapidly than $\alpha = 1/3$ predicts. We however assume that strong winds do not develop over most of the disk radius, and we adopt $\alpha = 1/3$ as a maximal value.

2. By identifying the precise boundary between gravitoturbulent and fragmenting disks, Gammie (2001) provides the means to discriminate stable mass accretion from the formation of new bound objects. A number of papers argue that the precise outcome of fragmentation depends sensitively on the thermal properties of the disk (e.g., Pickett et al. 2003); nevertheless the threshold for instability is given adequately by equation (16).

These insights reveal two points about Lin & Pringle’s simulations. First, they estimate in a reasonable fashion the dynamics of protostellar disks in their main accretion phase (since their estimate of α matched Gammie’s result when $Q = 1$); and second, that these disks are typically beyond the threshold for fragmentation.

The results of Gammie’s two-dimensional simulations (corroborated in three dimensions by Rice et al. 2003) provide a practical, local description for the disks that have entered a state of self-gravitating turbulence. This state separates disks that are relatively smooth from those that have fragmented into swarms of clumps; it also is a state in which the mean midplane conditions (density, temperature, etc.) are reasonably constrained. We use it as a litmus test for fragmentation in a variety of circumstances.

The following sections re-examine protostellar disk instability, connecting it to the core properties derived in §2 and examining why it is typical for protostellar cores to cross the threshold for fragmentation.

4.1. Local criteria for Toomre’s instability

Toomre (1964) demonstrated the onset of axisymmetric instability in disks with $Q < 1$; although other modes grow for somewhat higher Q , Gammie (2001)

verified that $Q \simeq 1$ at the boundary of fragmentation. This condition may immediately be expressed in terms of c_s , the midplane density ρ , and the midplane pressure p :

$$c_s = \frac{\pi G \Sigma}{\Omega}, \quad \rho = \frac{\Omega^2}{2\pi G}, \quad \text{and} \quad p = \frac{2}{\pi} G \Sigma^2, \quad (18)$$

where the middle expression uses the approximate relation $\rho = \Sigma \Omega / (2c_s)$, and the last expression uses $p = \rho c_s^2$. These relations are only approximate, as they neglect the disk's self-gravity (which is increasingly important as $Q \rightarrow 1$); nevertheless they do suffice to delineate the onset of instability.

An important additional criterion comes from combining eqs. (12), (15), and (17) to give

$$\frac{\dot{M}_{\text{visc}}}{\dot{M}_{\text{acc}}} = \frac{3\alpha}{\varepsilon Q} \frac{c_s^3}{c_{\text{eff}}^3}. \quad (19)$$

Gammie's simulations show that α attains a maximum of roughly 1/3 as Q drops slightly below unity and the local cooling time drops below roughly half the orbital period. Conversely, if the disk processes gas in steady state ($\dot{M}_{\text{visc}} = \dot{M}_{\text{acc}}$) then

$$Q = \frac{3\alpha}{\varepsilon} \frac{c_s^3}{c_{\text{eff}}^3}. \quad (\text{steady-state}) \quad (20)$$

The disk can therefore process steady accretion only when

$$c_s > \varepsilon^{1/3} c_{\text{eff}}, \quad (21)$$

i.e., using eq. (8) to describe a typical unstable core,

$$T > \varepsilon^{2/3} T_{\text{eff}} \simeq \frac{1.44}{f_p^{1/2}} \left(\frac{\varepsilon}{60\%} \right)^{2/3} T_c \quad (22)$$

(where T refers to the midplane temperature); otherwise fragmentation will occur where the gas falls. For typical core temperatures of order 10 K, disks colder than about 14 K unable to process the high accretion rate and will fragment into clumps.

4.1.1. Self-luminous disks

If the heat generated locally by viscosity is responsible for the midplane temperature, then criterion (21) may be evaluated directly. Our treatment follows Lin & Pringle (1990) and Levin (2003), among others. In thermal steady state, the flux of viscous

²Recently, Johnson & Gammie (2003) have published numerical experiments on razor-thin discs and have shown that Eq. (24) is generally inaccurate when the disc develops strong gravitationally-driven turbulence. However, in their model the breakdown of Eq. (24) is serious when the opacity is a sensitive function of temperature, which occurs only when the dust begins to evaporate at above 1000 K. Temperatures this high are clearly irrelevant for protostellar discs beyond a fraction of an AU, and thus for the problem at hand Eq. (24) is adequate. We also note that when the opacity is temperature sensitive, then the one-zone model of Johnson & Gammie does not treat faithfully the vertical radiative transport in a real disc.

energy radiated by each face of the disk is related to the accretion rate through

$$F_v = \frac{3\Omega^2 \dot{M}}{8\pi}. \quad (23)$$

The flux can also be derived from radiation transfer across an optical depth $\tau = \kappa \Sigma / 2$ from the disk midplane to its surface; therefore

$$F_r = \sigma T^4 \times \begin{cases} 4\tau_R & (\tau \ll 1) \\ 16/(3\tau_{\text{Pl}}), & (\tau \gg 1) \end{cases} \quad (24)$$

where $\tau_{R,\text{Pl}} = \kappa_{R,\text{Pl}} \Sigma / 2$ is the optical depth corresponding to Rosseland and Planck opacity, κ_R and κ_{Pl} , respectively.² The factor 16/3 arises in the optically thick case when the dissipation rate per unit mass is a constant (e.g., Chick & Cassen 1997) and is only approximate. For the disk to achieve an equilibrium temperature in which local heating balances radiative cooling, we must have $F_v = F_r$.

The midplane temperature and sound speed are related via

$$c_s^2 = \frac{k_B T}{\mu} \quad (25)$$

where $\mu \simeq 2.3m_p$ is the mean molecular weight. We neglect radiation pressure in this expression. This is entirely justified for present-day star formation, since when $Q = 1$,

$$\frac{p_{\text{gas}}}{p_{\text{rad}}} = \frac{2\pi G a \mu T^3}{3k\Omega^2} = 11 \left(\frac{1000 \text{ yr}}{\text{period}} \right)^2 \left(\frac{500 \text{ K}}{T} \right)^3$$

using eq. (18).

For the opacity we adopt

$$\begin{pmatrix} \kappa_R \\ \kappa_{\text{Pl}} \end{pmatrix} = \kappa_0 T^2 = \begin{pmatrix} 3.0 f_{\kappa R} \\ 8.4 f_{\kappa \text{Pl}} \end{pmatrix} \times 10^{-4} T^2 \text{ cm}^2 \text{ g}^{-1}. \quad (26)$$

This describes the ice branch of Semenov et al. (2003)'s ice grain opacities in their "composite aggregate" model; eq. (26) fits their results around 14 K. Note that Alexander & Ferguson (1994) computed somewhat lower opacities ($f_{\kappa R} \simeq 0.67$; see also Bell & Lin 1994). Henning & Stognienko (1996) also derive a lower value ($f_{\kappa R} \simeq 0.43$) after allowing for dust agglomeration in the parent molecular core. We include the two f_{κ} factors to account for variations in metallicity, dust processing, and uncertainties in opacity modeling.

Equations (23), (24), (25), and (26) provide enough information to solve $F_v = F_r$ for $T(r)$, given an accretion rate \dot{M} . As discussed above, the local accretion

rate (eq. [17]) must match the supply (eq. [12]). To determine the onset of fragmentation, we also impose $Q \rightarrow 1$ (eq. [15]). We find that fragmentation ensues when

$$\Omega = \Omega_{\text{cr}} \times \begin{cases} \left(\frac{c_{\text{eff}}}{c_{\tau}}\right)^{10}, & c_s < c_{s,\tau} (\tau \ll 1) \\ 1, & c_s > c_{s,\tau} (\tau \gg 1) \end{cases} \quad (27)$$

where

$$\begin{aligned} \Omega_{\text{cr}} &= 4.53 \left[\frac{G^2 \mu^2 \sigma}{\alpha \kappa_0 k_B^2} \right]^{1/3} \\ &= 5.7 \times 10^{-10} f_{\kappa R}^{-1/3} \left(\frac{\mu}{2.3 m_p} \right)^{2/3} \left(\frac{1/3}{\alpha} \right)^{1/3} \text{ s}^{-1}, \end{aligned} \quad (28)$$

corresponding to a period of 350 years for the fiducial parameters (306 years for Alexander & Ferguson's opacity; 264 years for Henning & Stognienko's opacity), and

$$c_{s,\tau} = \frac{0.185}{f_{\kappa R} f_{\kappa \text{Pl}}^{1/30}} \left(\frac{\alpha}{1/3} \right)^{1/15} \left(\frac{2.3 m_p}{\mu} \right)^{8/15} \text{ km s}^{-1} \quad (29)$$

To summarize, disks with opacity law (26) that are warmed solely by their own viscosity will be subject to local fragmentation in any region whose orbital frequency is less than the value given in eq. (27).

It is worthwhile to emphasize two points about the above equations. First, Ω_{cr} is an upper bound for the frequency of a locally unstable disk, i.e., all locally unstable disks have periods of roughly 350 years or longer. This bound depends *only* on the opacity law of the disk midplane and is independent of the mass supply rate and disk surface density (so long as the disk is optically thick). This result is specific to a cancellation that occurs when the opacity varies as T^2 .

Second, the lower bound on the period at which fragmentation can occur is pushed to even higher values if the disk is optically thin or if it is affected by external irradiation. We discuss below the case of optically thin discs and postpone the treatment of irradiation until the next section. The division between optically thin and thick fragmentation depends only on the midplane sound speed c_s ; the critical value $c_{s,\tau}$ corresponds to a midplane temperature of roughly 9.6 K. But recall that we already know the midplane temperature at which the disk cannot stably process accretion: $T = \varepsilon^{2/3} T_{\text{eff}}$ (eq. [22]), or ~ 14.4 K. Indeed, using equations (22) and (29), cores with

$$T_c > 6.7 \frac{f_p^{1/2}}{f_{\kappa \text{Pl}}^{1/5} f_{\kappa R}^{1/15}} \left(\frac{60\%}{\varepsilon} \right)^{2/3} \text{ K} \quad (30)$$

will produce disks that are significantly more prone to fragmentation than those from colder cores because of the transition to optically thick disks.

Suppose for the sake of illustration that the characteristic temperatures of protostellar cores were 5 K rather than 10 K. Then, the effective temperature (including turbulence) would be roughly 10.1 K (eq. [8], with $f_p = 1$), and disks would fragment once they cooled below 7.2 K (for $\varepsilon = 60\%$; eq. [21]). The disk would then be optically thin at the location of its fragmentation, since 7.2 K is below the requisite 9.6 K for optical thickness. The disk periods suitable for fragmentation would therefore be restricted to those exceeding $350(9.6 \text{ K}/7.2 \text{ K})^5 = 1,470$ years. That is, the disk would not fragment within about 130 AU. In contrast, cores of 7 K or higher have disks that are optically thick at the fragmentation radii and all of which can fragment where the period exceeds roughly 350 years (~ 50 AU).

As this example indicates, equations (27) – (29) imply that the cosmic thermal history of star-forming gas has a controlling influence on the disk fragmentation mechanism of stellar binary formation.

Equation (27) argues strongly against the formation of giant planets by direct disk fragmentation, in agreement with the recent work by Rafikov (2004). This argument gains strength when the effect of stellar irradiation is considered.

4.2. Irradiation

The preceding section identified a critical midplane temperature for local fragmentation (typically ~ 14 K in disks around low-mass protostars, eq. [22]), and a critical disk period (typ. ~ 350 yr) above which viscous heating permits cooler midplane temperatures. However as we mentioned before, the argument in the preceding section neglects external irradiation of the disc. Here we self-consistently take irradiation into account and show that it prevents completely the local fragmentation for a large range of core parameters.

To illustrate its importance, suppose irradiation normal to the disk surface is a fraction f_F of the spherical flux. The equilibrium temperature of an optically thick disk is then given by $\sigma T^4 = f_F L / (4\pi R_d^2)$, if L is the accretion luminosity; or

$$T = 120 f_F^{1/4} \left(\frac{T_{\star}}{4500} \right)^{1/3} \left(\frac{350 \text{ yr}}{\text{period}} \right)^{1/3} \left(\frac{\dot{M}_{\text{acc}}}{3 \times 10^{-6} M_{\odot} \text{ yr}^{-1}} \right)^{1/6} \quad (31)$$

where the stellar effective temperature is T_{\star} . (Note T is independent of the stellar mass M .) If the disk

is optically thin, its temperature is generically higher than given above: for a local radiation energy density is aT_{egy}^4 and color temperature is T_c , the equilibrium temperature of an optically thin region is

$$T^4 \kappa_{\text{Pl}}(T) = T_{\text{egy}}^4 \kappa_{\text{Pl}}(T_c) \quad (32)$$

where κ_{Pl} refers to the Planck average opacity. Since $T^4 \kappa_{\text{Pl}}(T)$ is monotonic, $T_{\text{egy}} < T < T_c$. Furthermore, since the flux at the disk surface cannot exceed $aT_{\text{egy}}^4 c$, an optically thin disk must be warmer than a thick disk in the same radiation environment.³

The flux suppression factor f_F can be quite small in the case that the disk is illuminated at a grazing incidence from the stellar photosphere (e.g., Kenyon & Hartmann 1987; Chiang & Goldreich 1997). For an accreting protostar, however, reradiation from the stellar envelope tends to illuminate and heat the disk (Keene & Masson 1990; Natta 1993; Chick et al. 1996; Chick & Cassen 1997; D'Alessio et al. 1997).

To gauge this, consider the column of the infall envelope. The spherically averaged column density outward from some radius r is $\Sigma_{\text{sph}}(r) = 2\dot{M}/[4\pi r^2 v_{\text{esc}}(r)]$. Evaluated at the centrifugal radius in eq. (13),

$$\Sigma_{\text{sph}}(R_d) = 0.43 \frac{\varepsilon}{60\%} \frac{f_p^{3/4}}{f_j} \Sigma_{\text{cl}}. \quad (33)$$

In spherical infall $\Sigma_{\text{sph}}(r)$ diverges inward as $r^{-1/2}$. For rotating infall, however, only low- j material persists within R_d ; this makes $\Sigma_{\text{sph}}(R_d)$ a characteristic value for the column *inward* from R_d , as well. Intriguingly, the column at R_d is comparable to that of the parent clump or cloud, Σ_{cl} , at the end of accretion. (Beforehand it is much greater: the column to the disk edge varies as t^{-2} during steady accretion.) Deviations from spherical symmetry due to angular momentum are given by the rotating-infall solution of Terebey et al. (1984). Additionally, the protostellar jet will scour the axis to produce a cavity.

The characteristic column $\Sigma_{\text{sph}}(R_d)$ is thus roughly $\Sigma_{\text{cl}}/2$, i.e., half that of the parent clump or cloud; starlight is absorbed and reprocessed after it traverses a fraction of this column. The reprocessing is strongly affected by the presence or absence of an outflow cavity: therefore, we consider both cases.

4.2.1. No outflow cavity

The reprocessing radius typically lies well inside R_d but outside the dust evaporation radius, because the

latter is optically thin in the end phases of accretion. Disk irradiation is therefore due primarily to the second reprocessing of starlight at radii around R_d . We shall identify the dust temperature at the reprocessing surface, which affects the amount of re-absorption and re-emission above the disk.

Close to the protostar, the angle-averaged column density in the Terebey et al. (1984) infall profile is $\bar{\Sigma}(r) = 1.17(r/R_d)^{1/2} \Sigma_{\text{sph}}(R_d) + \mathcal{O}(r/R_d)^{3/2}$. If we identify the reprocessing radius r_1 with the surface of optical depth unity, then $\bar{\Sigma}(r_1) \kappa_{\star} = 1$, where $\kappa_{\star} \equiv \kappa_{\text{Pl}}(T_{\star})$ is the opacity to starlight of color temperature T_{\star} . In addition, equation (32) determines the dust temperature T_1 at this location: $\kappa_{\text{Pl}}(T_1) T_1^4 = \kappa_{\star} L / (4\pi r_1^2 ac)$. Combining these,

$$\frac{\kappa_{\text{Pl}}(T_1)}{\kappa_{\star}^5} \sigma T_1^4 = \frac{L \Sigma_{\text{sph}}^4}{26.7}. \quad (34)$$

The left hand side is a somewhat complicated function of T_1 because the dust composition, a function of T_1 , determines κ_{\star} and $\kappa_{\text{Pl}}(T_1)$; metallicity and the stellar temperature T_{\star} also enter.⁴ The right hand side depends on model parameters. A self-consistent solution of (34) is not always available; this signals a change in the dust composition and fixes T_1 at a composition boundary. Nevertheless, this equation demonstrates that the reprocessing temperature T_1 is a pure function of $L \Sigma_{\text{sph}}^4$ for fixed T_{\star} and metallicity, so long as the infall is optically thick to starlight. In a range of T_1 for which the dust composition is constant, $T_1 \propto L^{1/6} \Sigma_{\text{sph}}^{2/3}$ because $\kappa_{\text{Pl}}(T_1) \propto T_1^2$.

Given a optically thin emission at the reprocessing temperature T_1 , the effective opacity for the second reprocessing event is given by

$$\bar{\kappa} = \frac{\int \kappa_{\nu 2} \kappa_{\nu 1} B_{\nu}(T_1)}{\int \kappa_{\nu 1} B_{\nu}(T_1)} \quad (35)$$

where $\kappa_{\nu 1}$ is the opacity law at the reprocessing radius and $\kappa_{\nu 2}$ is that for cool dust near R_d . Figure 1 shows T_1 and $\bar{\kappa}$ for a given model; notably, $\bar{\kappa} \simeq 15 \text{ cm}^2 \text{ g}^{-1}$ for a wide range of parameters, dropping only for especially large disk radii (and especially low values of $\Sigma_{\text{sph}}(R_d)$).

Integrating the flux through the disk at R_d from the sky intensity of reradiated light (assuming optically thin second reprocessing), we find that the flux of this radiation at the disk radius R_d is given by equation (31) if

$$f_F = 0.28 \bar{\kappa} \Sigma_{\text{sph}} \quad (36)$$

³The lower limit on T in the thin case is $\sqrt{2}$ below that in eq. (31), but this factor is not significant.

⁴ T_1 also depends weakly on the gas density at r_1 , which affects the evaporation temperatures of the dust components; this is ignored in eq. 34.

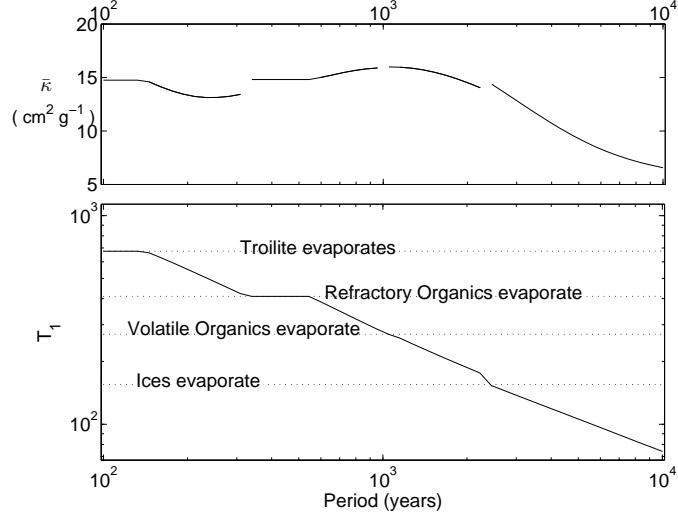


FIG. 1.— Lower panel: Temperature T_1 of the reprocessing surface in envelopes lacking outflow cavities. T_1 is computed as a function of outer disk period using the opacity model of Semenov et al. (2003). Assumed parameters are $M = 0.5M_\odot$, $M = 3 \times 10^{-6} M_\odot \text{ yr}^{-1}$, $T_* = 4500 \text{ K}$, and solar metallicity; however, equation (34) permits this diagram to be rescaled for other parameters. (The density dependence of evaporation temperatures has been suppressed for simplicity; lines here are drawn for $10^{-10} \text{ g cm}^{-3}$.) Upper panel: effective opacity $\bar{\kappa}$ of cool dust to optically thin thermal radiation from dust of temperature T_1 .

giving $f_F \simeq 1/16$ for typical parameters. Using this result to calculate the irradiation temperature in eq. (31), we find that it falls below the critical temperature for local fragmentation if

$$\text{period} > 1.2 \times 10^4 f_p^{9/20} \left(\frac{M_\odot}{M} \right)^{2/5} \left(\frac{\bar{\kappa}}{10 \text{ cm}^2 \text{ g}^{-1}} \right)^{3/5} \times \left(\frac{T_*}{4500 \text{ K}} \right)^{4/5} \left(\frac{10 \text{ K}}{T_c} \right)^{9/10} \text{ yr} \quad (37)$$

This indicates that local disk fragmentation is suppressed in the absence of an outflow cavity except for periods comparable to or greater than the maximum disk period identified in §2.2. Note we have taken $\varepsilon = 100\%$ here, since the absence of the outflow cavity implies that all of the material is accreted onto the star. This raises the critical disk temperature to about 20 K.

4.2.2. Outflow cavity

A more realistic calculation must account for the region along the axis that is cleared by the jet. To do so, we must specify the shape of the outflow cavity.

Note, first, that the wind ram pressure is expected generically to vary as $1/(r^2 \sin^2 \theta)$ with distance and angle θ from the axis (Matzner & McKee 1999). Inflow ram pressure scales as $r^{-5/2}$ from the centrifugal radius to the edge of the inflow. We see on comparison that inflow dominates close to the star and near the equator, and the wind dominates far from the star and near the axis. By this reasoning, Matzner & McKee (2000) divided the initial core into

accreting and ejected angles depending on the velocity imparted by the wind impulse to gas at the edge of the core. Our parameter ε is simply the accreted mass as a fraction of the initial mass.

By the same logic, gas that is not cast away by the wind is destined to fall inward, and its motion is less and less affected by the wind ram pressure as it does. Therefore we are justified in approximating the shape of the outflow cavity as an unperturbed streamline in the infall solution of Terebey et al. (1984). The streamline in question is roughly the one that divides infall and outflow in Matzner & McKee (2000)'s theory. For the case of a spherical initial core, then, the initial angle of this streamline is given by

$$\cos \theta_0 = \varepsilon. \quad (38)$$

(We shall assume a spherical core for the remainder of this section.) This streamline strikes the disk at a radius $\sin^2(\theta_0)R_d = (1 - \varepsilon^2)R_d$.

Geometrically, a fraction ε of the starlight strikes the cavity inner edge because the remaining $1 - \varepsilon$ is cleared by the outflow. However, smaller ε leads to a broader outflow cavity, which causes a greater portion of the reprocessed starlight to reach the disk. We find that f_F is adequately described by $0.1\varepsilon^{-0.35}$ in the relevant range $20\% < \varepsilon < 90\%$. The infall envelope is translucent to this reprocessed radiation, but our estimates indicate that shadowing of the disk by the infall is insufficient to change this result significantly.

The disk temperature at R_d exceeds the critical

value of ~ 14 K unless

$$\text{period} > 3.0 \times 10^4 f_p^{9/20} \left(\frac{60\%}{\varepsilon} \right)^{1.8} \frac{T_\star}{4500 \text{ K}} \left(\frac{10 \text{ K}}{T_c} \right)^{9/4} \text{ yr} \quad (39)$$

Finally, we note that the disk is optically thin to the reprocessed radiation, causing its midplane temperature to exceed that used in equations (37) and (39). This pushes the minimum periods for local fragmentation to nonphysically large values.

Consider now the evolution of the effect of irradiation as the accretion rate declines. The critical disk midplane temperature, eq. (22), varies as $\dot{M}_{\text{acc}}^{2/3}$. The radiative flux normal to the outer disk varies as the central luminosity ($\propto \dot{M}_{\text{acc}}$ for low-mass stars); if the infall is optically thin then there is another factor of \dot{M}_{acc} in the reprocessed fraction. The flux therefore varies as $\dot{M}_{\text{acc}}^{1-2}$, implying a midplane temperature that varies as $\dot{M}_{\text{acc}}^{0.25-0.5}$. The weaker dependence implies that a disk which is stabilized by irradiation will remain so as the mass supply wanes. This might not hold if accretion were to stop suddenly compared to the disk's viscous time, but this is not realistic.

To summarize, *local fragmentation due to Toomre's instability is quenched by irradiation in protostellar disks.*

5. GLOBAL INSTABILITY

In light of the previous section, one expects irradiation to prevent local fragmentation and possibly also to prevent the enhanced angular momentum transport from self-gravity. Note, however, that Gammie (2001)'s results were for razor-thin disks, and protostellar disks are rather thick in comparison. Therefore, the disk mass can become large enough to induce global instability. As we shall see, the threshold for this depends on the ability of local angular momentum transport (e.g., due to MRI) to remove material from the disk.

Adams et al. (1989) and Shu et al. (1990) describe a global "SLING" instability in which the disk becomes massive enough that the star is perturbed from the center of mass by the action of a lopsided spiral. Shu et al. (1990) provide the following formula (their eq. [111]) for the criterion of instability:

$$\frac{M_d}{M_d + M} = \frac{3}{4\pi} \mathcal{M}(Q) \quad (40)$$

where

$$\begin{aligned} \mathcal{M}(Q) &\equiv \int [x^4 + 4Q^2(x - x^{5/2})]^{1/2} dx \\ &\simeq 1 + \frac{8}{9}(Q - 1) \end{aligned} \quad (41)$$

where the approximation is exact in the limits $Q \rightarrow 1$ and $Q \rightarrow \infty$ and holds within 2.3% for all $Q > 1$.

When it sets in, this instability is thought to transport material rapidly enough to prevent fragmentation (Laughlin et al. 1998, see however Bonnell 1994).

We shall not posit $Q = 1$, because we have seen in §4.2 that irradiation tends to warm the disk so that $Q > 1$. Instead, let us assume $\Sigma \propto r^{-3/2}$ so that $M_d = 4\pi R_d^2 \Sigma$. If we approximate $\Omega^2 \rightarrow G(M + M_d)/R_d^3$ and retain $H = c_s/\Omega$, then (15) becomes

$$Q = 4 \frac{H}{r} \left(1 + \frac{M}{M_d} \right). \quad (42)$$

With equations (40) and (41), this gives a maximum stable disk mass as a function of H/r . We find that $Q > 1$ and $M_d < M$ requires $0.06 < H/r < 0.28$; within this range, we approximate the exact solution of equations (40), (41), and (42):

$$\frac{M_d}{M} < 3.09 \frac{H}{r} + 0.13 \quad (43)$$

for global stability. The approximation is valid within 1%.

This can be compared to the mass accumulated, which for $\Sigma \propto r^{-3/2}$ is

$$M_d = \frac{\dot{M}_{\text{acc}}}{\Omega} \frac{4}{3\alpha} \left(\frac{r}{H} \right)^2. \quad (44)$$

The comparison sets a minimum for α/α_0 , where

$$\alpha_0 \equiv \frac{\dot{M}_{\text{acc}}}{M\Omega}. \quad (45)$$

The theory of §2 indicates that

$$\alpha_0 = 10^{-2.6} \frac{f_j^3}{f_p^{3/4}} \left(\frac{60\%}{\varepsilon} \right)^2, \quad (46)$$

independently of the physical scale of the parent cloud.

Taken together, we find that the minimum α required to keep the disk stable can be approximated (within 4.2%)

$$\alpha > 0.52 \left(\frac{r}{H} \right)^{2.76} \alpha_0. \quad (47)$$

The instability is clearly very sensitive to the midplane temperature. Computing $H/r = c_s/v_k$ using the irradiation temperature model of §4.2.2 (which gives $H/r \sim 0.11$ for fiducial parameters), we find that stability requires

$$\begin{aligned} \alpha &> 0.19 \frac{f_j^{1.62}}{f_p^{1.27}} \left(\frac{60\%}{\varepsilon} \right)^{0.27} \left(\frac{T_c}{10 \text{ K}} \right)^{1.27} \\ &\times \left(\frac{165 M_\odot \text{ pc}^{-2}}{\Sigma_{\text{cl}}} \right)^{0.46} \left(\frac{4500}{T_\star} \right)^{0.46}. \end{aligned} \quad (48)$$

It has been argued that local gravitational transport becomes significant when Q falls below ~ 1.4 (Laughlin & Bodenheimer 1994). In its absence, the disk is left with magnetoturbulent (MRI) transport, which is thought to saturate at much lower values of α in a weakly ionized medium.

With eq. (48), this indicates that global spiral modes *can be* required for protostellar disks to process the mass supply, depending on the infall parameters and on the detailed irradiation temperature (which we have calculated only approximately). Disks that are especially thick or whose parent cores are especially slowly rotating ($f_j \ll 1$) will be stable at smaller values of α .

6. SUMMARY AND CONCLUSIONS

6.1. *Summary*

We derived in §2 a simple set of relations for the smallest and most thermally supported collapsible objects, i.e., cores, that can exist at a given mean gas temperature in a parent cloud of a given column density. The cloud column sets both the scale for the cores' bounding pressure, and the coefficient in the line width-size relation for cloud turbulence. This turbulence aids in core support and increases the minimum core mass, while also accelerating the accretion rate when cores do collapse (§2.2). In addition, turbulence bestows cores with rotational angular momentum that determines the characteristic scales for protostellar accretion disks (§2.1). This theory does not account for the role of a static magnetic field, nor does it prescribe the distribution of overpressures expected in a realistic model for molecular cloud turbulence; nevertheless, it matches the observations of prestellar cores of a couple solar masses (§2.4) with a minimum of free parameters. In our model, substellar cores would derive from regions of especially low temperature and high degrees of overpressure. High mass cores could come from the opposite conditions or, more likely, derive the bulk of their initial support from nonthermal pressure.

Turning next to the fragmentation boundary as predicted even in axisymmetric models of protostellar collapse, we found in §3 that the cores are typically subject to a phase of prompt fragmentation according to Matsumoto & Hanawa (2003)'s criterion. This is a possible mechanism for the production of relatively tight binary stars. However, we note that this occurs before most of the core mass has accreted; therefore these fragments may be driven to merge by radiating angular momentum to the accretion disk.

Examining the local gravitational stability of protostellar disks in §4.1, we made extensive use of the simulations by Gammie (2001) to identify a critical disk temperature that divides accreting from fragmenting

disks. For disks heated solely and locally by their own viscosity, we found in §4.1.1 that local fragmentation is impossible for disk periods shorter than about 350 years (depending on the opacity law), and that fragmentation is suppressed until much longer periods if the disk is optically thin to its own cooling radiation. This conclusion is entirely consistent with the recent argument by Rafikov (2004) that the formation of giant planets by direct disk instability (Boss 1997) is impossible on thermodynamic grounds. Moreover, when we account for heating by the star's accretion luminosity (reprocessed by the infall envelope), we find that the local instability is entirely quenched. A decline in the accretion rate does not alter this conclusion.

Lastly, we consider the onset of global instability due to the accumulation of a finite disk mass. Applying the instability criterion of Shu et al. (1990), we find that the intrinsic viscosity parameter α (e.g., due to MRI) must exceed $\sim 10^{-2}$ in order to prevent global instability. When it does occur, this instability is likely to saturate and provide rapid angular momentum transport rather than fragmentation (Laughlin et al. 1998).

6.2. *Conclusions: Stellar Binaries and the Brown Dwarf Desert*

Our foremost conclusion is that stellar and substellar companions are not produced by disk fragmentation. This indicates that turbulent perturbations beyond rotation and compression are responsible for the production of binary stars (Klein et al. 2003). Since companions formed in disk instabilities would be initially of substellar mass, this closes a formation channel for substellar companions. Observations (e.g., McCarthy & Zuckerman 2004) show a marked dearth of companions in the mass range between stars and planets – a brown dwarf desert. Armitage & Bonnell (2002) have ascribed this to inward disk migration that destroys brown dwarfs. However this presupposes that they can form within disks; here we have argued that they cannot.

Barrado y Navascués et al. (2004) argue from their observations of disk accretion onto free-floating brown dwarfs that these must form in isolation rather than from fragmentation in a disk or in a collapsing turbulent core. Our theoretical results also argue against a disk origin for these objects.

We thank Jonathan Williams, Ue-Li Pen, and Fred Adams for helpful and encouraging discussions; Mary Barsony and Sukanya Chakrabarti for useful comments; Roman Rafikov for pointing us to his preprint; and Dmitry Semenov for explanations concerning the Semenov et al. (2003) opacity model. CDM's re-

search is funded by NSERC and the Canada Research Chairs program. YL is supported by an NSERC se-

nior CITA postdoc.

References

Adams, F. C., Ruden, S. P., & Shu, F. H. 1989, *ApJ*, 347, 959

Alexander, D. R. & Ferguson, J. W. 1994, *ApJ*, 437, 879

Armitage, P. J. & Bonnell, I. A. 2002, *MNRAS*, 330, L11

Barrado y Navascués, D., Mohanty, S., & Jayawardhana, R. 2004, *ApJ*, 604, 284

Bell, K. R. & Lin, D. N. C. 1994, *ApJ*, 427, 987

Benson, P. J. & Myers, P. C. 1989, *ApJS*, 71, 89

Bonnell, I. A. 1994, *MNRAS*, 269, 837

Bonnor, W. B. 1956, *MNRAS*, 116, 351

Boss, A. P. 1997, *Science*, 276, 1836

Boss, A. P., Fisher, R. T., Klein, R. I., & McKee, C. F. 2000, *ApJ*, 528, 325

Burkert, A. & Bodenheimer, P. 2000, *ApJ*, 543, 822

Cameron, A. G. W. 1978, *Moon and Planets*, 18, 5

Chiang, E. I. & Goldreich, P. 1997, *ApJ*, 490, 368

Chick, K. M. & Cassen, P. 1997, *ApJ*, 477, 398

Chick, K. M., Pollack, J. B., & Cassen, P. 1996, *ApJ*, 461, 956

Crutcher, R. M., Nutter, D. J., Ward-Thompson, D., & Kirk, J. M. 2004, *ApJ*, 600, 279

Curry, C. & McKee, C. F. 1999

D'Alessio, P., Calvet, N., & Hartmann, L. 1997, *ApJ*, 474, 397

Duquennoy, A. & Mayor, M. 1991, *A&A*, 248, 485

Fisher, R. T. 2004, *ApJ*, 600, 769

Fuller, G. A. & Myers, P. C. 1993, *ApJ*, 418, 273

Gammie, C. F. 2001, *ApJ*, 553, 174

Goodman, A. A., Benson, P. J., Fuller, G. A., & Myers, P. C. 1993, *ApJ*, 406, 528

Goodman, J. 2003, *MNRAS*, 339, 937

Hennebelle, P., Whitworth, A. P., Gladwin, P. P., & André, P. 2003, *MNRAS*, 340, 870

Henning, T. & Stognienko, R. 1996, *A&A*, 311, 291

Hoyle, F. 1953, *ApJ*, 118, 513

Johnson, B. M. & Gammie, C. F. 2003, *ApJ*, 597, 131

Johnstone, D., Fich, M., Mitchell, G. F., & Moriarty-Schieven, G. 2001, *ApJ*, 559, 307

Keene, J. & Masson, C. R. 1990, *ApJ*, 355, 635

Kenyon, S. J. & Hartmann, L. 1987, *ApJ*, 323, 714

Klein, R. I., Fisher, R. T., Krumholz, M. R., & McKee, C. F. 2003, in *Revista Mexicana de Astronomia y Astrofisica Conference Series*, 92–96

Larson, R. B. 1981, *MNRAS*, 194, 809

Laughlin, G. & Bodenheimer, P. 1994, *ApJ*, 436, 335

Laughlin, G., Korchagin, V., & Adams, F. C. 1998, *ApJ*, 504, 945

Laughlin, G. & Rozyczka, M. 1996, *ApJ*, 456, 279

Levin, Y. 2003, ArXiv Astrophysics e-prints (astro-ph/0307084)

Lin, D. N. C. & Pringle, J. E. 1987, *MNRAS*, 225, 607

—. 1990, *ApJ*, 358, 515

Lodato, G. & Rice, W. K. M. 2004, *MNRAS*, 351, 630

Mac Low, M.-M. 1999, *ApJ*, 524, 169

Matsumoto, T. & Hanawa, T. 2003, *ApJ*, 595, 913

Matzner, C. D. & McKee, C. F. 1999, *ApJ*, 526, L109

—. 2000, *ApJ*, 545, 364

Mayer, L., Quinn, T., Wadsley, J., & Stadel, J. 2002, *Science*, 298, 1756

McCarthy, C. & Zuckerman, B. 2004, *AJ*, 127, 2871

McKee, C. F. 1999, in *NATO ASIC Proc. 540: The Origin of Stars and Planetary Systems*, 29

McKee, C. F. & Holliman, John H., I. 1999, *ApJ*, 522, 313

McKee, C. F. & Tan, J. C. 2003, *ApJ*, 585, 850

McKee, C. F. & Zweibel, E. G. 1995, *ApJ*, 440, 686

McKee, C. F., Zweibel, E. G., Goodman, A. A., & Heiles, C. 1993, in *Protostars and Planets*, 327

Motoyama, K. & Yoshida, T. 2003, *MNRAS*, 344, 461

Motte, F., André, P., & Neri, R. 1998, *A&A*, 336, 150

Myers, P. C. & Fuller, G. A. 1992, *ApJ*, 396, 631 ak

Natta, A. 1993, *ApJ*, 412, 761

Nelson, A. F., Benz, W., & Ruzmaikina, T. V. 2000, *ApJ*, 529, 357

Paczynski, B. 1978, *Acta Astronomica*, 28, 91

Padoan, P. & Nordlund, Å. 2002, *ApJ*, 576, 870

Padoan, P., Nordlund, A., & Jones, B. J. T. 1997, *MNRAS*, 288, 145

Pak, S., Jaffe, D. T., Van Dishoeck, E. F., Johansson, L. E. B., & Booth, R. S. 1998, *ApJ*, 498, 735

Papaloizou, J. C. & Savonije, G. J. 1991, *MNRAS*, 248, 353

Pickett, B. K., Mejía, A. C., Durisen, R. H., Cassen, P. M., Berry, D. K., & Link, R. P. 2003, *ApJ*, 590, 1060

Plume, R., Jaffe, D. T., Evans, N. J., I., Martin-Pintado, J., & Gomez-Gonzalez, J. 1997, ApJ, 476, 730

Rafikov, R. 2004, ArXiv Astrophysics e-prints (astro-ph/0406469)

Rice, W. K. M., Armitage, P. J., Bate, M. R., & Bonnell, I. A. 2003, MNRAS, 339, 1025

Rosolowsky, E., Engargiola, G., Plambeck, R., & Blitz, L. 2003, ArXiv Astrophysics e-prints

Sargent, A. & Scoville, N. 1991, ApJ, 366, L1

Scoville, N. Z., Sargent, A. I., Sanders, D. B., & Soifer, B. T. 1991, ApJ, 366, L5

Semenov, D., Henning, T., Helling, C., Ilgner, M., & Sedlmayr, E. 2003, A&A, 410, 611

Shakura, N. I. & Sunyaev, R. A. 1973, A&A, 24, 337

Shu, F. H. 1977, ApJ, 214, 488

Shu, F. H., Tremaine, S., Adams, F. C., & Ruden, S. P. 1990, ApJ, 358, 495

Solomon, P. M., Rivolo, A. R., Barrett, J., & Yahil, A. 1987, ApJ, 319, 730

Stone, J. M., Ostriker, E. C., & Gammie, C. F. 1998, ApJ, 508, L99

Terebey, S., Shu, F. H., & Cassen, P. 1984, ApJ, 286, 529

Tohline, J. E. 1994, in Physics of Accretion Disks Around Compact and Young Stars, 9–10

Tohline, J. E. 2002, ARA&A, 40, 349

Toomre, A. 1964, ApJ, 139, 1217

Truelove, J. K., Klein, R. I., McKee, C. F., Holliman, J. H., Howell, L. H., Greenough, J. A., Howell, L. H., & Greenough, J. A. 1997, ApJ, 489, L179+

Visser, A. E., Richer, J. S., & Chandler, C. J. 2002, AJ, 124, 2756

Zweibel, E. G. & Josafatsson, K. 1983, ApJ, 270, 511

APPENDIX

SPECIFIC ANGULAR MOMENTUM DISTRIBUTION OF PRESTELLAR CORES

We now compute the angular momentum distribution quoted in equations (10) and (11) according to the model for core rotation described in §2.1. Since we are interested in the specific angular momentum normalized to $R\sigma_{\text{NT}}(R)$, we compute the numerator and denominator separately.

Angular momentum

To calculate the angular momentum we assume, as a starting point, that the velocity difference between the two points scales as a square root of the distance between the points. More precisely,

$$\langle [v_i(r_1) - v_j(r_2)]^2 \rangle = k|\mathbf{r}_1 - \mathbf{r}_2|\delta_{ij} \quad (\text{A1})$$

where we assume that $|r_1 - r_2| \ll v^2/k$ if $v = \langle |\mathbf{v}|^2 \rangle^{1/2}$ is the characteristic turbulent velocity. Equation (A1) is assumed to hold for each velocity component v_i independently. We can then write down the correlation function for the velocity components:

$$\langle v_i(r_1)v_j(r_2) \rangle = \left(\frac{1}{3}v^2 - \frac{1}{2}k|\mathbf{r}_1 - \mathbf{r}_2| \right) \delta_{ij}. \quad (\text{A2})$$

Skipping to the result, the core's root mean square angular momentum is given by

$$\langle L^2 \rangle^{1/2} = 2\pi k^{1/2} R^{9/2} \rho_0 [F(\bar{\rho})]^{1/2}, \quad (\text{A3})$$

where R is the core radius and ρ_0 is the core density at the center; $\bar{\rho}(\bar{r}) = \rho(r)/\rho_0$ is the spherically symmetric normalized density profile expressed in terms of the dimensionless radius $\bar{r} = r/R$, and the form factor F is given by the following double integral:

$$\begin{aligned} F = & \int_0^1 \int_0^1 d\bar{r}_1 d\bar{r}_2 \bar{\rho}(\bar{r}_1) \bar{\rho}(\bar{r}_2) \bar{r}_1 \bar{r}_2 (\bar{r}_1^2 + \bar{r}_2^2)^{5/2} \times \\ & \left\{ \frac{1}{5} \left[(1+q)^{5/2} - (1-q)^{5/2} \right] \right. \\ & \left. - \frac{1}{3} \left[(1+q)^{3/2} - (1-q)^{3/2} \right] \right\}. \end{aligned} \quad (\text{A4})$$

Here $q = 2r_1 r_2 / (r_1^2 + r_2^2)$.

Evaluated over a Bonnor-Ebert sphere, $F^{1/2} = 0.0294$. Such spheres obey $M = 0.735\rho_0 R^3$, so that

$$\langle j^2 \rangle^{1/2} = \frac{\langle L^2 \rangle^{1/2}}{M} = 0.251 k^{1/2} R^{3/2}. \quad (\text{A5})$$

The derivation is as follows. The total angular momentum is given by

$$L^2 = L_x^2 + L_y^2 + L_z^2. \quad (\text{A6})$$

By spherical symmetry the components of angular momentum are uncorrelated; this can be checked directly. Therefore,

$$\langle L^2 \rangle = 3\langle L_z^2 \rangle = 3\langle (L_1 - L_2)^2 \rangle, \quad (\text{A7})$$

where

$$L_1 = \int d^3 \mathbf{r} \rho(r) x v_y, \quad (\text{A8})$$

$$L_2 = \int d^3 \mathbf{r} \rho(r) y v_x \quad (\text{A9})$$

But $\langle L_1 L_2 \rangle = 0$ and, by spherical symmetry, $\langle L_1^2 \rangle = \langle L_2^2 \rangle$. Therefore,

$$\begin{aligned} \langle L^2 \rangle &= 6\langle L_1^2 \rangle \\ &= 6 \int \int d^3 \mathbf{r}_1 d^3 \mathbf{r}_2 \rho(r_1) \rho(r_2) x_1 x_2 \langle v_y(\mathbf{r}_1) v_y(\mathbf{r}_2) \rangle. \end{aligned} \quad (\text{A10})$$

We can now use Eq. (A2) and evaluate the integral above. First, note that only the second term on the right-hand side of Eq. (A2) contributes to the integral. Second, because of the spherical symmetry we can substitute $x_1 x_2$ by $(\mathbf{r}_1 \mathbf{r}_2)/3$ in the integrand. Thus we have for the total angular momentum:

$$\langle L^2 \rangle = -k \int \int d^3 \mathbf{r}_1 d^3 \mathbf{r}_2 \rho(r_1) \rho(r_2) (\mathbf{r}_1 \mathbf{r}_2) |\mathbf{r}_1 - \mathbf{r}_2|. \quad (\text{A11})$$

The integrand in Eq. (A11) depends only on the magnitudes of \mathbf{r}_1 and \mathbf{r}_2 , and on the angle θ between them. Therefore, the other three free variables are integrated out, and we are left with the 3-d integral:

$$\begin{aligned} \langle L^2 \rangle &= -k \int dr_1 4\pi r_1^2 \rho(r_1) \times \\ &\quad \int \int dr_2 2\pi d \cos \theta \cos \theta \left[\rho(r_2) r_1 r_2 \sqrt{r_1^2 + r_2^2} \right. \\ &\quad \left. \sqrt{1 - q \cos \theta} \right], \end{aligned} \quad (\text{A12})$$

where

$$q = \frac{2r_1 r_2}{r_1^2 + r_2^2}. \quad (\text{A13})$$

The angular integration in Eq. (A12) can be performed analytically, most simply by using $\sqrt{1 - q \cos \theta}$ as an integration variable. The result of this calculation is presented in Equations (A3) and (A4).

One-dimensional velocity dispersion

We now compute the one-dimensional velocity dispersion:

$$\begin{aligned}\sigma^2 &= \int d^3\mathbf{r} \tilde{\rho} [v_x(\mathbf{r}) - \bar{v}_x]^2 \\ &= \int d^3\mathbf{r} \tilde{\rho} [v_x(\mathbf{r})^2 - 2v_x(\mathbf{r})\bar{v}_x + \bar{v}_x^2] \\ &= \left[\int d^3\mathbf{r} \tilde{\rho} v_x(\mathbf{r})^2 \right] - \bar{v}_x^2\end{aligned}\quad (\text{A14})$$

where $\tilde{\rho} \equiv \rho/M$ and \bar{v} denotes the center of mass velocity:

$$\bar{v} = \int d^3\mathbf{r} \tilde{\rho} v(\mathbf{r}) \quad (\text{A15})$$

In equation (A14), the first term reduces after ensemble averaging to $v^2/3$, according to equation (A2). Likewise for the second term,

$$\begin{aligned}\langle \bar{v}_x^2 \rangle &= \int \int d^3\mathbf{r}_1 d^3\mathbf{r}_2 \tilde{\rho}(\mathbf{r}_1) \tilde{\rho}(\mathbf{r}_2) \langle v_x(\mathbf{r}_1) v_x(\mathbf{r}_2) \rangle \\ &= \int \int d^3\mathbf{r}_1 d^3\mathbf{r}_2 \tilde{\rho}(\mathbf{r}_1) \tilde{\rho}(\mathbf{r}_2) \left(\frac{1}{3} v^2 - \frac{1}{2} k |\mathbf{r}_1 - \mathbf{r}_2| \right).\end{aligned}\quad (\text{A16})$$

The constant terms cancel in the ensemble average of eq. (A14), leaving

$$\begin{aligned}\langle \sigma^2 \rangle &= \frac{1}{2} k \int \int d^3\mathbf{r}_1 d^3\mathbf{r}_2 \tilde{\rho}(\mathbf{r}_1) \tilde{\rho}(\mathbf{r}_2) |\mathbf{r}_1 - \mathbf{r}_2| \\ &= \frac{1}{2} k \int 4\pi r_1^2 dr_1 \tilde{\rho}(r_1) \int 2\pi r_2^2 \tilde{\rho}(r_2) \sqrt{r_1^2 + r_2^2} \times \\ &\quad \int d\cos\theta \sqrt{1 - q \cos\theta} \\ &= \frac{8\pi^2}{3} k R \int \int d\bar{r}_1 d\bar{r}_2 \bar{r}_1^2 \bar{r}_2^2 \tilde{\rho}(\bar{r}_1) \tilde{\rho}(\bar{r}_2) \sqrt{\bar{r}_1^2 + \bar{r}_2^2} \times \\ &\quad [(1+q)^{3/2} - (1-q)^{3/2}].\end{aligned}\quad (\text{A17})$$

Evaluated over a Bonnor-Ebert sphere,

$$\langle \sigma^2 \rangle^{1/2} = 0.607 k^{1/2} R^{1/2}, \quad (\text{A18})$$

and in combination with equation (A5),

$$\langle j^2 \rangle^{1/2} = 0.414 \langle \sigma^2 \rangle^{1/2} R. \quad (\text{A19})$$

Since the velocity distribution is Gaussian, all of its linear moments (e.g., L_x and σ) are Gaussian distributed. The cumulative probability distribution of j , $\mathcal{P}(< j)$, is therefore Maxwellian with a width fixed by equation (A19):

$$\frac{d\mathcal{P}(< j)}{d(j/\langle j^2 \rangle^{1/2})} = 3 \sqrt{\frac{6}{\pi}} \frac{j^2}{\langle j^2 \rangle} \exp\left(-\frac{3j^2}{2\langle j^2 \rangle}\right) \quad (\text{A20})$$

A log-normal fit to this distribution is $\log_{10} j/\langle j^2 \rangle^{1/2} = -0.080 \pm 0.52$, but this is not especially accurate. A more faithful representation is $\log_{10} j/\langle j^2 \rangle^{1/2} = -0.088_{-0.49}^{+0.16}$.